CHEMISTRY
A EUROPEAN JOURNAL

DOI: 10.1002/chem.201000466

Vectorial Photoinduced Energy Transfer Between Boron–Dipyrromethene (Bodipy) Chromophores Across a Fluorene Bridge**

Fausto Puntoriero,[a] Francesco Nastasi,[a] Sebastiano Campagna,*[a] Thomas Bura,[b] and Raymond Ziessel*[b]

Abstract: A series of novel multichromophoric, luminescent compounds has been prepared, and their absorption spectra, luminescence properties (both at 77 K in rigid matrix and at 298 K in fluid solution), and photoinduced intercomponent energy-transfer processes have been studied. The series contains two new multichromophoric systems **1** and **2**, each one containing two different boron–dipyrromethene (Bodipy) subunits and one bridging fluorene species, and two fluorene–Bodipy bichromophoric species, **6** and **7**. Three monochromophoric compounds, **3**, **4**, and **5**, used as precursors in the synthetic process, were also fully characterized. The absorption spectra of the multichromophoric compounds are roughly the summation of the absorption spectra of their individual components, thus demonstrating the supramolecular nature of the assemblies. Luminescence studies show that quantitative energy transfer occurs in **6** and **7** from the fluorene chromophore to the Bodipy dyes. Luminescence studies, complemented by transient-absorption spectroscopy studies, also indicate that efficient inter-Bodipy energy transfer across the rigid fluorene spacer takes place in **1** and **2**, with rate constants, evaluated by several experimental methods, between 2.0 and $7.0\times10^{9}\ s^{-1}$. Such an inter-Bodipy energy transfer appears to be governed by the Förster mechanism. By taking advantage of the presence of various protonable sites in the substituents of the lower-energy Bodipy subunit of **1** and **2**, the effect of protonation on the energy-transfer rates has also been investigated. The results suggest that control of energy-transfer rate and efficiency of inter-Bodipy energy transfer in this type of systems can be achieved by an external, reversible input.

Keywords: boron · energy transfer · fluorene · luminescence · multicomponent reactions

Introduction

Photoinduced energy transfer has been studied for several decades[1] and continues to attract increasing attention since it plays key roles in both natural and artificial systems dealing with the conversion of light energy into more concentrated forms of energy (i.e., electrical[2] and chemical energy[3]) and/or information technology.[4]

Recently, much of that attention has been concentrated on organized, supramolecular assemblies, in particular on multichromophoric systems in which vectorial electronic energy transfer (EET) is maximized across a rigid spacer that keeps the chromophores far apart.[5] The role of the rigid spacer is not limited to a structural one, but it can also be active in assisting the EET process by means of superexchange,[6] particularly if the Dexter electron exchange mechanism[7] significantly contributes to the process. Furthermore, multichromophoric assemblies for vectorial EET in which the efficiency and rate of the photoinduced energy-transfer process can be controlled are highly desirable, since

[a] F. Puntoriero, F. Nastasi, S. Campagna
Dipartimento di Chimica Inorganica
Chimica Analitica e Chimica Fisica
Università di Messina and Centro Interuniversitario
per la Conversione Chimica dell'Energia Solare (sede di Messina)
Via Sperone 31, 98166 Vill. S. Agata, Messina (Italy)
Fax: (+39) 090-393756
E-mail: campagna@unime.it

[b] T. Bura, R. Ziessel
Laboratoire de Chimie Organique et Spectroscopies Avancées (LCOSA)
Centre National de la Recherche Scientifique (CNRS)
Ecole de Chimie, Polymères Matériaux (ECPM)
Université de Strasbourg (UdS)
25 rue Becquerel, 67087 Strasbourg Cedex 02 (France)
Fax: (+33) 390-242689
E-mail: ziessel@unistra.fr
Homepage: http://www-lmspc.u-strasbg.fr/lcosa

[**] Bodipy = 4,4-difluoro-4-bora-3a,4a-diaza-*s*-indacene.

Supporting information for this article is available on the WWW under http://dx.doi.org/10.1002/chem.201000466. It includes Figures SI1–SI4, which show a comparison of absorption spectra, excitation spectra, and titration processes.

such systems could have a large importance for future developments in several areas, including information technology based on controlled light impulse.

Over the last decade, fluorene, oligofluorene, and polyfluorene derivatives have emerged as a promising class of blue-light-emitting materials for use in polymer-based emissive displays, organic light-emitting devices, and solar cells mostly because of high photoluminescent and electroluminescent yields.[8,9] These properties could easily be tuned through chemical structure modification, and an impressive set of chemical tools are now available to modify the fluorene backbone at will.[10] Along these lines, we have previously prepared fluorene derivatives chemically modified in the 2,7-substitution positions by protected alkyne fragments.[11] These stable building blocks appeared interesting in the construction of phosphorescent architectures based on transition metals. In the present contribution, the central fluorene subunit has been modified in the central 9,9′-substitution position to connect a short ethyleneglycol chain and to insure good solvent solubility and to import polarity, a key tenet for purification purposes. The π-conjugated tethers were introduced at the 2,7-position by means of acetylene chemistry using palladium(0) cross-coupling reactions.

The use of 4,4-difluoro-4-bora-3a,4a-diaza-*s*-indacene (Bodipy) dyes has recently become very popular as a result of their valuable optical properties.[12] Among these, pronounced stability, a high absorption coefficient in the visible portion of the electromagnetic spectrum, narrow emission profiles, and outstanding emission quantum yields approaching 100% are available in the best cases. A cornerstone of these particular dyes is the possibility to react the methyl residue at the *ortho* position of the dipyrromethene core, to increase the π conjugation, and to adequately tune absorption and fluorescence properties. From these capabilities numerous applications have emerged, such as use in solar concentrators, artificial molecular scale wires,[13] multichromophoric scaffoldings dedicated to directional energy transfer,[14] solar cells,[15] fluorescence-sensing materials,[16] probes for biolabeling,[17] as well as laser applications.[18] In some limited cases, engineering allowed for the production of two-photon-absorbing dyes dedicated to cell imaging.[19] Recently, new types of liquid crystals,[20] fluorescent organogelators,[21] and controlled polymers have been produced by tailoring specific decoration at the periphery of the dyes.[22]

Here we report two new multicomponent species, **1** and **2** (see structural formulae in Scheme 1), each of them containing two different Bodipy dyes connected by a rigid fluorene bridging subunit. The absorption spectra and luminescence properties of the multichromophoric assemblies and the vec-

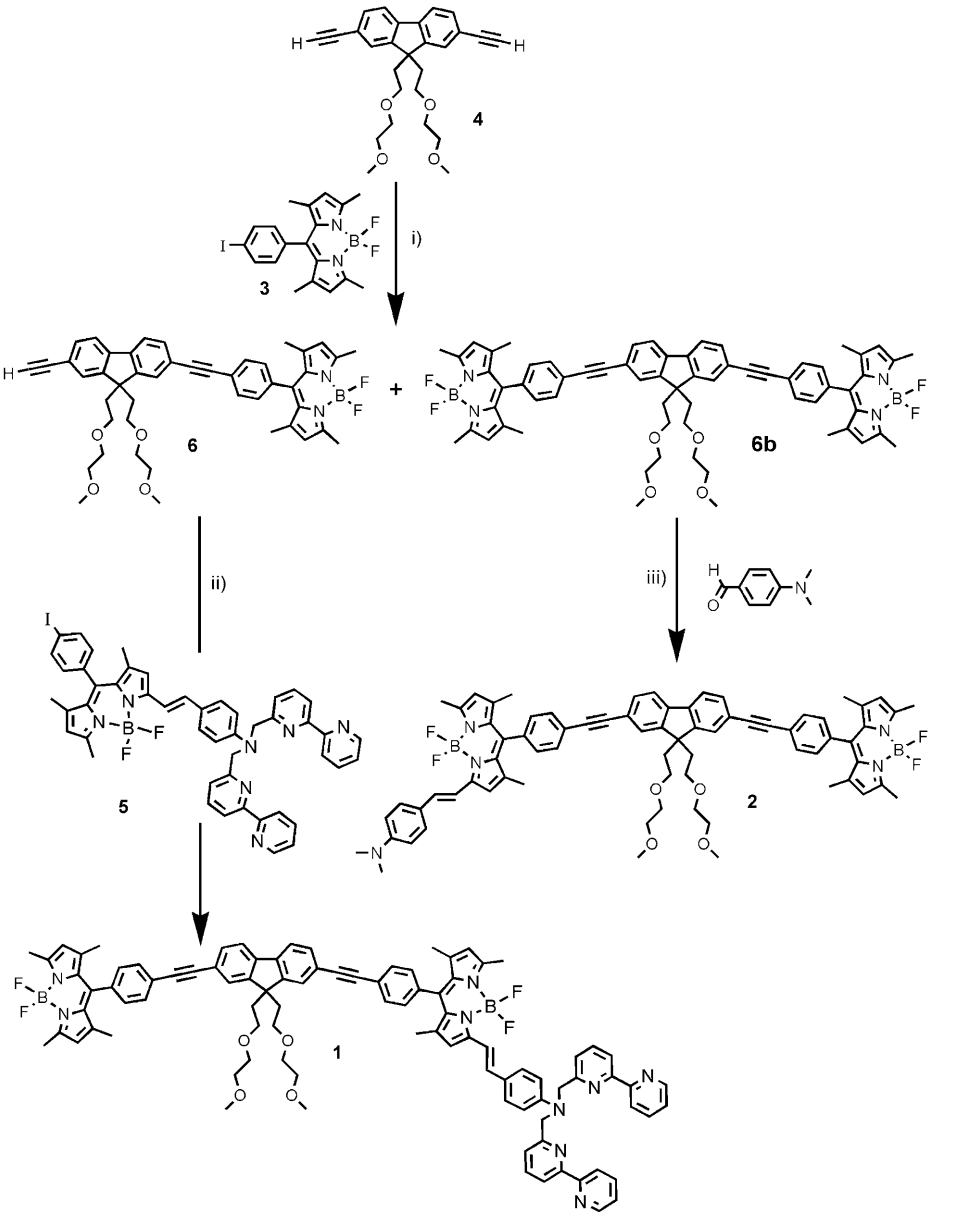

Scheme 1. i) Compound **3** (1 equiv), $[Pd(PPh_3)_4]$ (10 mol%), C_6H_6/Et_3N, 60°C, 15 h, 25% of **6b**, 21% of **6**; ii) compound **5** (1 equiv), $[Pd(PPh_3)_4]$ (10 mol%), C_6H_6/Et_3N, 60°C, 15 h, 42%; iii) 4-dimethylbenzaldehyde (1 equiv), toluene, piperidine, Dean Stark, trace *p*-TsOH, 45%.

torial photoinduced energy-transfer processes that occur between Bodipy subunits in **1** and **2** across the bis-(ethynyl)fluorene bridge have been investigated, together with the absorption spectra and luminescence properties of the four model compounds **4**, **5**, **6**, and **7**, also shown in Scheme 1. Furthermore, by taking advantage of the possible protonation of the pendant aminostyryl substituents of the acceptor Bodipy subunits of **1** and **2**, we also show that a reversible perturbation (protonation/deprotonation) can affect the rate constant and efficiency of the EET process in the studied compounds.

Results

The target compounds **1** and **2** were prepared as shown in Scheme 1. The pivotal diethynylfluorene compound **4** was prepared in three steps from 2,7-dibromofluorene and carries two ethyleneglycol chains at the central five-membered ring. The cross-coupling reaction between compound **4** and the Bodipy dye **3**[23] is promoted by palladium(0) in the presence of a base, which quenches the nascent acid generated during the reaction. This statistical reaction afforded the mono-Bodipy dye **6** and the disubstituted derivative **6b**. Both compounds were easily separated by column chromatography thanks to the presence of two short ethyleneglycol chains. A second cross-coupling was realized using the blue dye **5**[24] and the fluorene-substituted Bodipy dye **6** under our standard experimental conditions, thereby providing the mixed dye **1** in 42% after purification. The bis-Bodipy dye **6b** was reacted with 4-dimethylaminobenzaldehyde to afford the mixed dye **2** in 45% isolated yield. This Knoevenagel reaction,[25] catalyzed by piperidine under heating at reflux and following protocols established earlier,[26] was inspired by previous work on linear Bodipy molecular-scale wires.[27] Noteworthy is the fact that no degradation or multisubstitution was observed under standard conditions. Here the polarity is imported by the dimethylamino fragment, which facilitates the purification process. As would be expected by the type of condensation employed, an *E* conformation of the double bond was found as revealed by the observed $J = 16.4$ Hz proton–proton coupling constant in the proton NMR spectra.[28] Finally, the model compound **7** was prepared in 40% by cross-coupling the blue dye **5** to compound 2-ethynyl-7-trimethylsilylacetylene-9,9-bis[2-(2-methoxyethoxy)ethyl]fluorene, itself obtained as a side product from the deprotection process that leads to compound **4** (Scheme 2). These new compounds were characterized unambiguously by NMR spectroscopic studies, ESIMS, as well as by elemental analysis, which support the supposed stoichiometry when double substitution is feasible.

The absorption spectra of solutions of compounds **1**, **2**, **4**, **5**, **6**, and **7** in acetonitrile at room temperature show intense bands both in the UV and in the visible region (with the exception of **4**, which only exhibits absorption in the UV region). In most cases, the absorption bands are structured. The relevant data is collected in Table 1, and Figure 1,

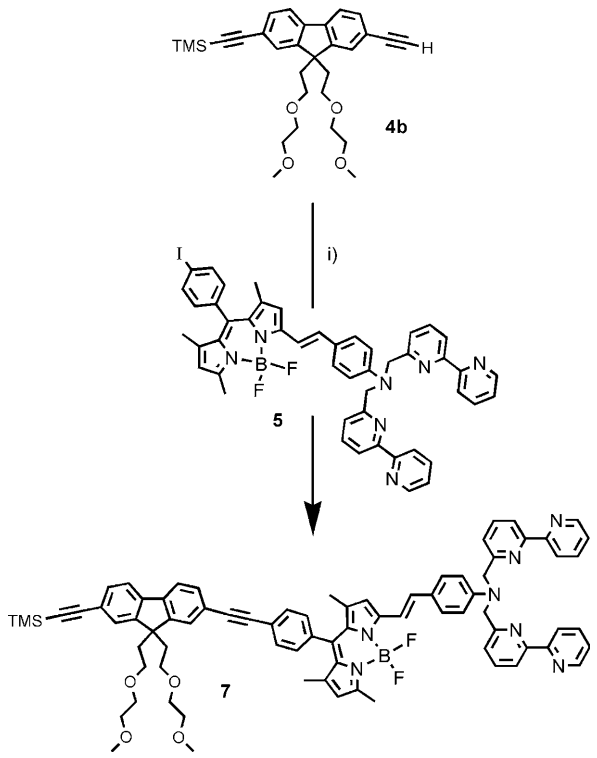

Scheme 2. i) Compound **5** (1 equiv), $[Pd(PPh_3)_4]$ (10 mol%), THF/Et_3N, 60°C, 15 h, 40%.

Table 1. Absorption and luminescence data of the studied complexes. Data are for samples in acetonitrile unless otherwise stated.

Compound	Absorption[a]	Luminescence				
	λ_{max} [nm]	298 K			77 K[b]	
	(ε [$M^{-1}cm^{-1}$])	λ_{max} [nm]	τ [ns]	Φ	λ_{max} [nm]	τ [ns]
1	600 (75000)	695	2.22[c]	0.26[d]	630	3.30
	500 (75000)	510	0.16[e]	0.06[f]	510	0.40
	355 (88000)	–	–	–	–	–
2	605 (75000)	725	0.80[c]	0.15[d]	655	4.00
	500 (75000)	510	0.20[e]	0.07[f]	510	0.45
	355 (92000)	–	–	–	–	–
4	326 (55000)	333	1.51	0.70	332	1.60
	302 (51000)					
5	600 (75000)	695	2.00	0.26	633	3.80
	385 (17000)					
	290 (34000)					
6	500 (70000)	510	1.80	0.39	510	5.30
	335 (60000)					
	230 (37000)					
7	600 (75000)	695	2.00	0.26	633	3.20
	340 (65000)					
	290 (42000)					

[a] Only the maxima of the main absorption bands are given. [b] In butyronitrile rigid matrix; please note that all the data are identical to those obtained in MeOH/EtOH 4:1 (v/v), not shown. [c] Measured in the lower-energy emission band. [d] Quantum yield obtained by exciting in the lowest-energy absorption band. [e] Measured in the higher-energy emission band. [f] Quantum yield obtained by exciting at 480 nm, at which point absorption is almost exclusively due to the higher-energy Bodipy dye (see text).

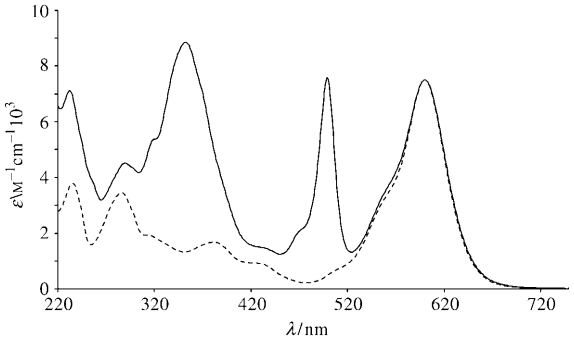

Figure 1. Absorption spectra of solutions of **1** (——) and **5** (-----) in acetonitrile.

Figure 2, and Figure 3 show the absorption spectra of all the compounds.

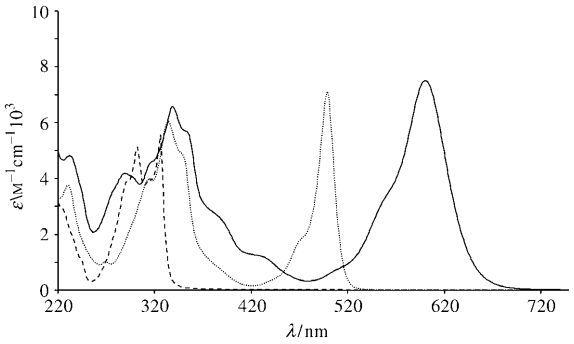

Figure 2. Absorption spectra of solutions of **4** (-----), **6** (•••••), and **7** (——) in acetonitrile.

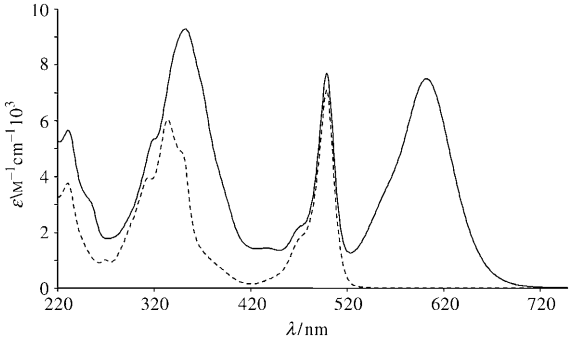

Figure 3. Absorption spectra of solutions of **2** (——) and **6** (——) in acetonitrile.

All the studied compounds exhibit luminescence both at room temperature in acetonitrile and at 77 K in butyronitrile and MeOH/EtOH 4:1 (v/v) rigid matrices. In all cases, compounds **4**–**7** show a single luminescence feature, which in most cases exhibits a vibrational progression with monoexponential decays; both compounds **1** and **2** exhibit two luminescence features, which decay with different lifetimes. For the latter two compounds, luminescence spectra are also slightly excitation-wavelength dependent, with the higher-energy emission slightly increased when short-wavelength excitation is used, whereas the luminescence spectra are independent from excitation wavelength for the other studied compounds. Figure 4 shows the room temperature emission spectra of **4**, **6**, and **7**, Figure 5 shows the room temperature emission spectra of **1** and **2**, excited at different wavelengths, and Figure 6 shows the 77 K emission spectra of all compounds. Luminescence spectra maxima, luminescence lifetimes, and quantum yields of all the studied compounds are gathered in Table 1.

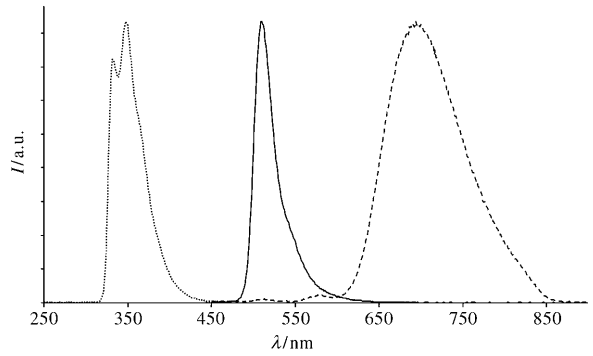

Figure 4. Emission spectra of solutions of **4** (•••••), **6** (——), and **7** (-----) in acetonitrile at room temperature.

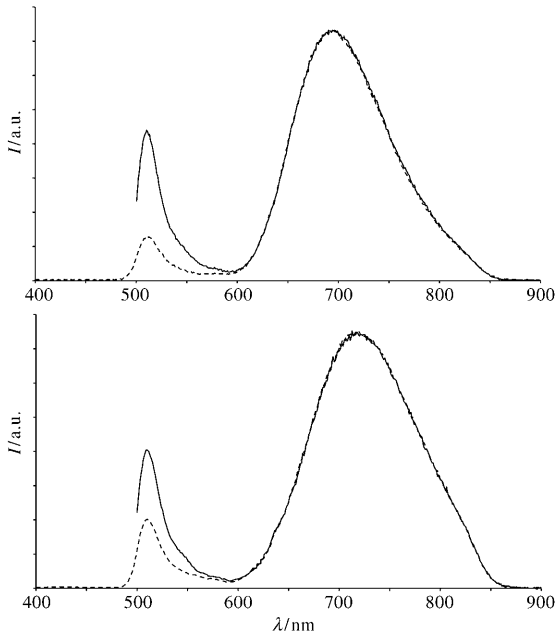

Figure 5. Normalized emission spectra of **1** (top panel) and **2** (bottom) in acetonitrile at room temperature. Excitation is 480 nm (——) or 335/350 nm (-----).

Transient absorption spectra have been performed on solutions of **1** and **2** in acetonitrile at room temperature, on exciting at 400 nm (see Figure 7 for compound **1**). For both **1** and **2**, two main bleachings are formed immediately after

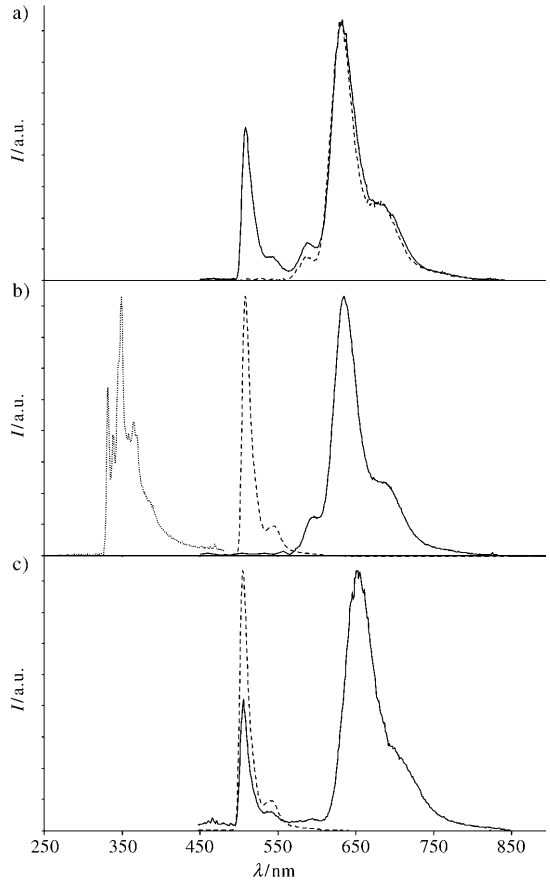

Figure 6. Emission spectra of the studied compounds in a butyronitrile rigid matrix at 77 K. a) **1** (——) and **5** (-----). b) **4** (•••••), **6** (-----), and **7** (——). c) **2** (——) and **6** (-----). Compounds **1** and **2** are excited at 480 nm. The spectra of the other species are independent of excitation wavelength.

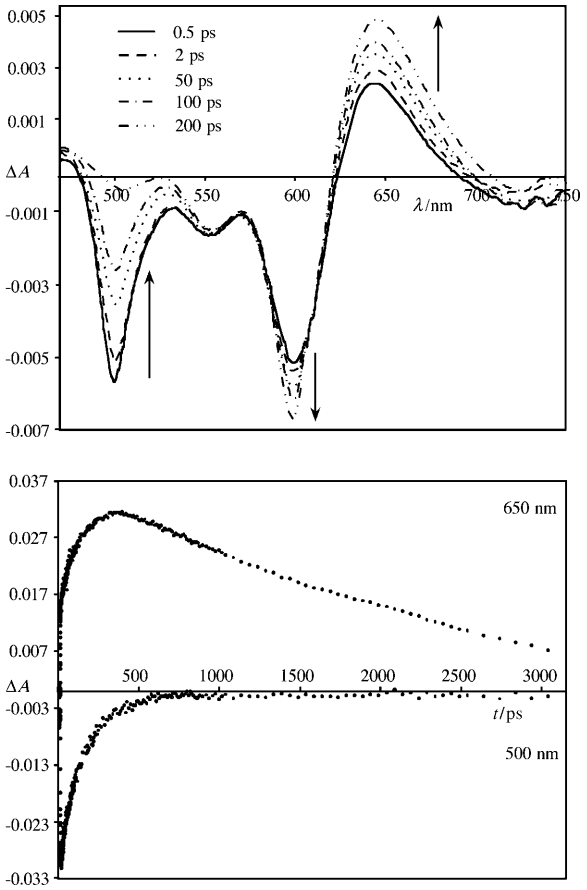

Figure 7. Top panel: transient absorption spectra of **1** in acetonitrile (excitation 400 nm). The spectra registered between 0.5 and 200 ps are shown. In the bottom panel, kinetic traces at 650 and 500 nm (complete time range) are shown.

excitation: the bleaching at higher energy (in the range 450–520 nm) is recovered on the picosecond timescale and simultaneously the bleaching at lower energy (in the range 560–610 nm) increases, coupled with a transient absorption growing at wavelengths longer than 620 nm. The low-energy bleaching is then recovered on a longer timescale (ns), together with the decay of transient absorption at wavelengths longer than 620 nm.

Discussion

Absorption spectra: Because of the large values of molar absorption (Table 1), the main absorption bands of the compounds can be assigned to spin-allowed π–π* transitions. It appears that the absorption spectra of the multichromophoric species are roughly the sum of the absorption spectra of the individual components (an example is shown in Figure SI-1 of the Supporting Information, which shows a comparison of the absorption spectrum of **1** with that obtained by the sum of the absorption spectra of **5** and **6**).

In particular, a careful comparison of the absorption spectra (see Figures 1–3) allows us to state that the fluorene chromophore **4** (which is also present in **2**, **6**, and **7**) has its main absorption in the range 260–350 nm; the Bodipy species that does not contain aminostyryl substituents, present in **6** (and also present in the multichromophoric species **1** and **2**), exhibits its main absorption feature in the region around 450–520 nm; the aminostyryl-substituted Bodipy chromophore, which is present in **1**, **5**, **7**, and although slightly modified in **2**, has its main absorption band in the 520–650 nm range. However, whereas the bands assigned to the absorption features of fluorene derivative **4** and to the Bodipy chromophores that do not bear aminostyryl substituents are clearly structured, it can be noted that the absorption bands due to the aminostyryl-substituted Bodipy chromophore(s) are broader and the structural vibration is less pronounced. This suggests some charge-transfer (CT) contribution to the Bodipy-based lowest-energy absorption band of **1**, **2**, **5**, and **7**. However, such a contribution is probably relatively weak, as reported by Baruah et al.[29] for the quite related dye **A**, and definitely less pronounced than in the truxene-containing Bodipy **B**, the lowest-energy absorption

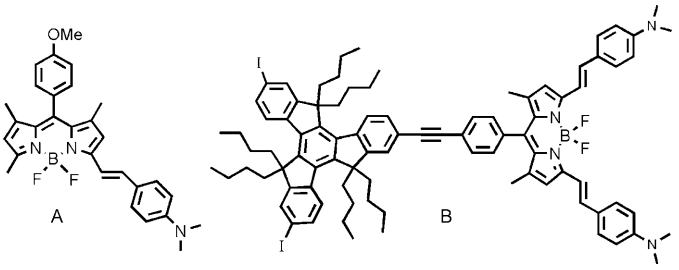

band of which is of dominant CT nature and in fact peaks at noticeably lower energy of 710 nm (in dichloromethane).[14]

Luminescence properties and photoinduced energy-transfer processes: The luminescence exhibited by **4** is straightforwardly assigned to fluorescence from its lowest-energy π–π* levels, as indicated by the small Stokes shifts (see Table 1, Figure 4), the structured shape of the emission band, the short lifetime, the high quantum yield, and the independence of the maximum of the emission on passing from a room-temperature solution in acetonitrile to 77 K (Table 1, Figure 6); a better resolved vibrational structure is also evident in the emission spectrum at 77 K, in full agreement with the π–π* emission assignment. The luminescence of **5** would also be straightforward to assign, as this species is a monochromophoric compound that contains an aminostyryl-substituted Bodipy molecule: however, the room-temperature emission spectrum of this species is broader than those reported for "non-aminostyryl-substituted" Bodipy molecules,[14] and is significantly blueshifted on passing from room-temperature fluid solution to 77 K rigid matrix (Table 1). Such features allow us to attribute the Bodipy-based emission of **5** to an excited state with a significant CT nature (from the amino group to the Bodipy subunit), as also reported for other aminostyryl-substituted Bodipy chromophores.[14,29]

Both compounds **6** and **7** contain two chromophores, the fluorene and the Bodipy subunits, therefore in principle they could exhibit two emission features. However, in both cases only the lowest-lying, Bodipy-based emission is found, both at room temperature and at 77 K (Table 1, Figure 4 and Figure 6). Excitation spectra of **6** and **7** (see the Supporting Information) show contributions from both fluorene-based and Bodipy-based absorption bands, so it can be assumed that quantitative energy transfer from the higher-energy fluorene subunit to the lower-energy Bodipy subunit takes place in these species. The emissive excited state of **7**, analogously to what was mentioned above for **5**, also exhibits a CT character, at least at room temperature.

Compounds **1** and **2** are both made of three chromophores, a bridging fluorene subunit, and two peripheral Bodipy-based chromophores (see structural formulae in Scheme 1). In both cases, the aminostyryl-substituted Bodipy molecule is the lowest-lying chromophore of the whole assembly. As expected on the basis of the luminescence properties of **6** and **7**, the bis-ethynylfluorene dye does not exhibit any luminescence, since it is efficiently quenched by energy transfer to the two peripheral Bodipy chromophores. In both **1** and **2**, two emission bands are evident (Table 1, Figure 5), which corresponds to the emission of the higher-energy (non-aminostyryl-substituted) and lower-energy (aminostyryl-substituted) Bodipy subunits. However, both in **1** and **2**, emission from the higher-energy Bodipy chromophore derived from **6** is strongly reduced relative to the corresponding emission of **6** (see Table 1). For example, in **1**, whereas the luminescence quantum yield of the lower-energy chromophore (calculated by integrating the emission intensity between 600 and 900 nm and exciting at 580 nm, in which absorption is exclusively due to the aminostyryl-substituted Bodipy subunit) is 0.26, identical to that of the parent species **7**, the emission quantum yield of the higher-energy Bodipy (calculated by integrating the emission intensity in the range 480–600 nm) is 0.06 upon exciting at 480 nm (at which point absorption is almost exclusively due to the higher-energy Bodipy) and is reduced to 0.03 upon exciting at 335 nm (at which excitation is largely fluorene-based, which can deactivate to both the peripheral Bodipy subunits), which is in any case quite reduced relative to the quantum yield of **6** (0.39). The room-temperature lifetime of the 500 nm emission band is 160 ps, which is also quite shorter than the luminescence lifetime of **6** (1.8 ns). Since the excitation spectra of **1** and **2** collected at the emission wavelength of the lowest-energy Bodipy subunit(s) fairly overlap with the respective absorption spectra (see Figure SI-2 in the Supporting Information), we can attribute the reduced emission of the higher-energy Bodipy subunit in **1** and **2** to an efficient, vectorial photoinduced energy transfer to the lower-energy Bodipy subunit(s) across the fluorene bridge.

As far as the rate constants of the energy-transfer processes in **1** and **2** are concerned, they can be calculated from the experimental luminescence lifetime and quantum yield data by Equations (1) and (2):

$$k_{en} = \frac{\frac{\Phi^0}{\Phi} - 1}{\tau^0} \quad (1)$$

$$k_{en} = \frac{1}{\tau'} - \frac{1}{\tau^0} \quad (2)$$

In Equations (1) and (2), Φ^0 and Φ are the unquenched and quenched quantum yields, respectively, and τ^0 and τ' are the unquenched and quenched lifetimes, respectively.[30] From Equation (1), the rate constant k_{en} of the higher-energy Bodipy to lower-energy Bodipy energy transfer in **1** is $3.1\times10^9\ s^{-1}$, whereas by using Equation (2), the resulting k_{en} is $5.7\times10^9\ s^{-1}$ (see Table 2). On considering the experimental uncertainties of lifetime (10%) and quantum yield (20%) measurements, such values appear to be in acceptable agreement with one another. As far as **2** is concerned, the calculated k_{en} values are 2.5×10^9 and $4.5\times10^9\ s^{-1}$ when Equations (1) and (2), respectively, are used. Also in this

Table 2. Rate constants k_{en} [s^{-1}] of the photoinduced inter-Bodipy energy-transfer process in **1** and **2** in acetonitrile at room temperature and at 77 K in a rigid matrix (sixth column), calculated by different methods, and other relevant data.

	k_{en} [Eq. (2)][a]	k_{en} (transient data)[b]	k_{en} [Eq. (3)][c]	J_F [cm^6][d]	k_{en} [Eq. (2)] 77 K	ΔG [eV][e]
1	5.7×10^9	6.7×10^9	9.7×10^9	1.10×10^{-13}	2.3×10^9	0.46
2	4.5×10^9	2.8×10^9	9.9×10^9	1.12×10^{-13}	2.0×10^9	0.54

[a] From luminescence experiments. Equation (1) yields slightly slower rate constants, but values from Equation (2) are considered more reliable (see text and ref. [31]), therefore these are the values derived from luminescence properties that we reported in Table 1. [b] From transient absorption spectroscopy. [c] From theory (approximated Förster equation). In the approximation, donor–acceptor distance is assumed to be 26.85 Å, taking into account the CT nature of the acceptor chromophore (for details, see text). [d] Spectral overlap integral used for the theoretical calculation of k_{en} expressed as in Equation (4). [e] Driving force of the energy transfer, approximated from the 77 K emission maxima of the partners (Table 1).

case, the agreement between the lifetime- and quantum-yield-derived values is considered acceptable.[31]

Inter-Bodipy photoinduced energy transfer in **1** and **2** also takes place at 77 K in a rigid matrix. Indeed, luminescence of the higher-energy Bodipy is significantly reduced in lifetime in the multi-Bodipy species relative to the model compound **6** (see Table 1). Rate constants of the intercomponent quenching process, calculated by using Equation (2) (Table 2), are of the same order of magnitude as those measured at room temperature and confirm the energy-transfer nature of the quenching mechanism.

Definitive support for the occurrence of the inter-Bodipy energy transfer in **1** and **2** are offered by transient absorption spectroscopy (Figure 7). Because of technical reasons, we were forced to perform ultrafast excitation only at 400 nm: at this wavelength both the peripheral Bodipy chromophores that are present in **1** and **2** absorb, therefore selective excitation is not possible. However, clear-cut conclusions could still be drawn. Ultrafast excitation of **1** at 400 nm leads to formation of both excited states that involve the two peripheral Bodipy dyes. The central fluorene chromophore is not excited since its absorption is negligible at this wavelength. The two excited states of the different Bodipy chromophores are signaled by the appearance of two bleachings in the differential absorption spectra recorded 400 fs after the flash (see Figure 7): the bleaching around 500 nm is clearly assigned to the excited state involving the higher-energy Bodipy subunit, and the bleaching at about 600 nm is assigned to the excited state that involves the lower-energy, aminostyryl-substituted Bodipy subunit. This transient spectrum evolves with time, thus leading to a recovery of the 500 nm bleach coupled with an enhanced bleaching at 600 nm. These two spectral changes are clearly concomitant, as shown by the almost identical time constants measured for the 500 nm bleaching recovery (130 ps) and for the 580 nm bleaching formation (170 ps). These results demonstrate that inter-Bodipy energy transfer takes place with a rate constant of about $6.7\times10^9\ s^{-1}$ (150 ps), which is in quite good agreement with luminescence data (see above; energy-transfer rate constants, derived from different methods, are collected in Table 2). Moreover, a transient absorption grows at a longer wavelength with a time constant (160 ps) that correlates with the energy-transfer process: this transient is therefore assigned to the lowest-energy Bodipy-based excited state of CT nature. The transient absorption spectrum of **1** successively decays on the nanosecond timescale, in agreement with luminescence data (Table 1). Figure 8 schematizes the EET process that occurs in **1**.

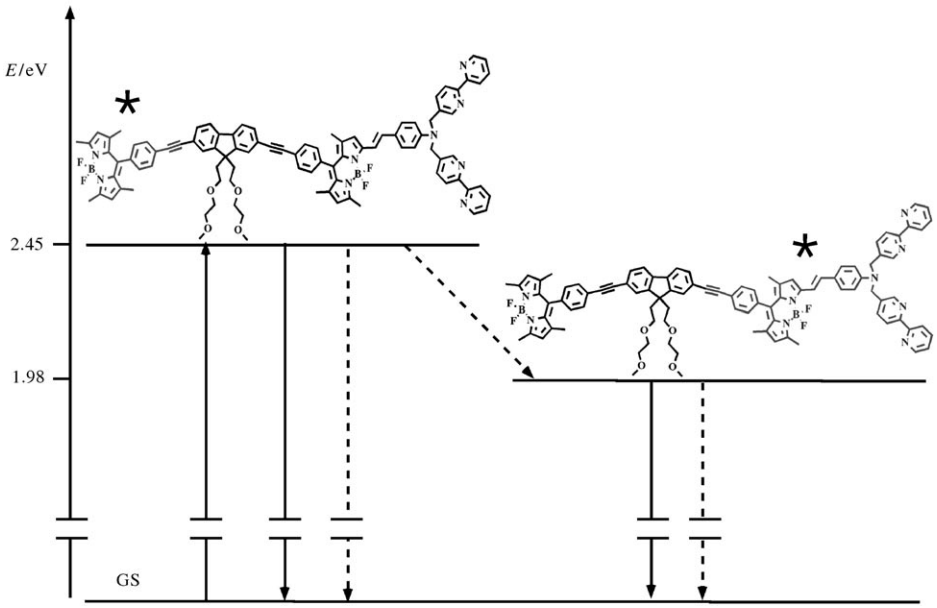

Figure 8. Energy-level diagram schematizing the energy-transfer process in **1**. GS stands for ground state. In the excited states, the asterisk indicates the Bodipy subunit at which the excited-state energy is located. Solid and dashed lines stand for radiative and radiationless transitions, respectively. The excited-state energies are approximated to the 77 K emission maxima (see Table 1) of the two Bodipy subunits.

An essentially identical situation can be discussed for **2** (not shown). In this case, the rate constant for the energy-transfer process derived from transient data is $2.8\times10^9\ s^{-1}$, still in fair agreement with luminescence data.

As far as the mechanisms of the energy-transfer processes that occur in the studied compounds are concerned, we

refer to the two main mechanisms usually invoked to explain EET between weakly coupled partners, that is, the Förster-type (Coulombic) resonance[32] and the Dexter-type electron exchange.[7]

The luminescence data of **6** and **7** show that the energy-transfer processes that occur in these species (that is, EET from the fluorene-based excited state to the lower-energy Bodipy-based chromophore(s)) are extremely fast, since the luminescence of the fluorene subunit, reported in **4**, is totally quenched, with concomitant sensitization of the Bodipy emission (see above). Since the diethynylfluorene and Bodipy(s) chromophores are quite close and directly linked (see Scheme 1), we assume that the Dexter electron exchange mechanism is responsible for the fast energy-transfer processes, although a Förster contribution cannot be excluded.

The situation is different for the inter-Bodipy energy-transfer processes that occur in **1** and **2**. In these cases, donor and acceptor chromophores are spatially separated by a bridge (the fluorene subunit) and the long-range Förster mechanism seems probable. Theoretical values for the energy-transfer rate constant by means of the Förster mechanism can be approximately obtained by using Equation (3),[33] in which k_{en}^{F} is the rate constant of the energy-transfer process; K is an orientation factor that accounts for the directional nature of the dipole–dipole interaction (K^2 is $^2/_3$ for random orientation); Φ and τ are the luminescence quantum yield and lifetime of the donor, respectively; n is the solvent refractive index; r_{AB} is the distance (in Å) between donor and acceptor; and J_F [see Eq. (4)] is the Förster overlap integral between the luminescence spectrum of the donor, $F(\bar{\nu})$, and the absorption spectrum of the acceptor, $\varepsilon(\bar{\nu})$, on an energy scale (cm^{-1}).

$$k_{en}^{F} = 8.8 \times 10^{-25} \frac{K^2 \Phi}{n^4 r_{AB}^6 \tau} J_F \quad (3)$$

$$J_F = \frac{\int F(\bar{\nu})\varepsilon(\bar{\nu})/\bar{\nu}^4 d\bar{\nu}}{\int F(\bar{\nu}) d\bar{\nu}} \quad (4)$$

It should be noted that Equation (3) (and its usual approximations mentioned above, including the average figure assumed for the dipole orientation factor) is a roughly approximated model of the Coulombic interaction between weakly interacting chromophores, and although this level of approximation allows in most cases satisfactory results, it can require modifications in several cases.[13,34,35]

For the inter-Bodipy energy transfer in **1** and **2**, in a first approximation for the donor–acceptor distance r_{AB} we assumed a value of 22.4 Å, which is the space distance between the center of the two dipyrromethene subunits, calculated from energy-minimized computer-generated structures. More precisely, it is the distance between the carbon atoms that connect two pyrroles in different dipyrromethene dyes. Since each Bodipy subunit is freely rotating along the triple-bond axis, a random value for the orientation factor (0.667) is assumed. The spectral overlap integral J_F results are almost identical for **1** and **2** (1.10×10^{-13} and 1.12×10^{-13} cm^6, respectively).

With the above-mentioned approximations, Equation (3) yields 2.9×10^{10} and 3.0×10^{10} s^{-1} as k_r values for **1** and **2** (Table 2), respectively. These rate constants are in both cases substantially larger than the experimental values. Such a discrepancy could mainly be due to the donor–acceptor distance we assumed between the Bodipy subunits in **1** and **2**: in fact, the acceptor partner of the energy-transfer process in both **1** and **2** (which is also partly responsible for the absorption spectra of the acceptor partner) is an excited state that has a significant CT level, so it is "delocalized" between the amino group and dipyrromethene framework of the aminostyryl-substituted Bodipy chromophore. This certainly modifies the donor–acceptor distance parameter:[36] if we add to the distance of separation between the carbon atoms that connect two pyrrole molecules in different Bodipy dyes mentioned above, halfway between the dipyrromethene framework and the amino group a donor–acceptor distance of 26.85 Å is obtained, and by using this value as the corrected r_{AB}, the calculated Förster rate constants for the energy-transfer processes that occur in **1** and **2** result in values of 9.7×10^9 and 9.9×10^9 s^{-1}, respectively, which are in much better agreement with the experimental values (see Table 2). However, whereas it appears that approximations on the calculated Förster rate constants by using Equation (3) limit the precise determination of such values, it can be safely stated that the mechanism of the inter-Bodipy EET in the studied species is Coulombic, Förster-type energy transfer.

Protonation effects on the inter-Bodipy energy-transfer processes: Bodipy compounds that contain aminostyryl groups are known to exhibit luminescence properties that strongly depend, reversibly, on protonation.[14,28,29,37] This is the case for the Bodipy species **A** and **B**, formerly discussed, the emissions of which are significantly blueshifted and enhanced upon proton addition, both in solution and in the solid state.[28,37] For such species, the lowest-energy absorption band also moves to higher energies upon protonation.[28,29] Since the absorption features of the aminostyryl Bodipy molecules have important roles in determining the energy-transfer rate constants in **1** and **2**,[38] it can be foreseen that the addition of protons can affect the efficiency of the photoinduced EET processes in **1** and **2**, so protons could play the role of promoters (or inhibitors) of the energy-transfer process, with the final result of opening the possibility of controlling the process by an external, reversible input.

The addition of triflic acid to a solution of **2** in acetonitrile (concentration: 3×10^{-6} M) leads to absorption and emission spectra changes that indicate complete protonation of the amino group at a 4:1 acid/**2** molar ratio; titration indeed evidences a series of isosbestic points, with the lowest-energy absorption band (Figure 9) moving to the blue, as expected.[28,29] The luminescence spectrum also moves to higher energy and the intensity of the low-energy emission (excita-

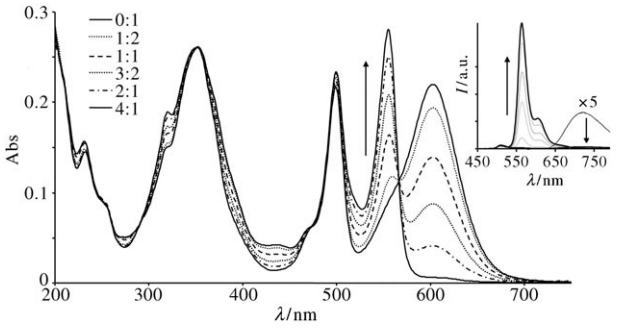

Figure 9. Absorption spectra changes of **2** upon protonation. Concentration of **2** is 3×10^{-6} M; in the panel, the molar ratio between added triflic acid and **2** is reported. The inset shows the changes on emission spectra (excitation at an isosbestic point, 480 nm) before and after titration.

tion wavelength, 480 nm) is significantly enhanced (Figure 9, inset). Interestingly, the absorption spectral features connected to the higher-energy Bodipy at about 500 nm are not modified appreciably by protonation, so confirming the expectation that the protonation process here monitored does not involve the higher-energy Bodipy. However, Specfit analysis of the titration followed by means of absorption spectrum changes indicates that two protons are involved, thereby forming a **2**·$(2H)^{2+}$ species. The two association constants k_1 and k_2 of the two protonation processes are apparently so close that they cannot be solved, and the global value for $\log k$ $(=\log k_1+\log k_2)$ for the **2**·$(2H)^{2+}$ species thus formed is 13.9 (with $(k_1+k_2)=8\times10^{13}\,M^{-2}$).

The luminescence lifetime of the higher-emission component of **2** is reduced upon protonation. In particular, the lifetime of the 500 nm emission, which was 200 ps in the absence of protons (see Table 1), become 140 ps for the **2**·$(2H)^{2+}$ species, which suggests an increase in energy-transfer rate constant (in spite of the reduced driving force, due to the shift to higher energy of the acceptor chromophore as shown by the inset of Figure 9), which in the protonated compound results to be $6.5\times10^{9}\,s^{-1}$ by using Equation (2) (to be compared with the $4.5\times10^{9}\,s^{-1}$ value obtained for the unprotonated species from emission lifetime measurements; the same method, based on Equation (2), is used for calculating energy-transfer rate constants, to have a homogeneous comparison). Luminescence quantum yield of the chromophore emissive at 500 nm is also affected by protonation: in fact, it decreases to about 60% of the value of the unprotonated compound (0.04 vs. 0.07). Therefore, luminescence data indicate that inter-Bodipy photoinduced energy transfer in **2** is accelerated by about 40% upon protonation.

The situation is quite different for **1**. Since this species contains an aminostyryl-substituted Bodipy that bears additional, potentially protonable units such as the two bipyridine moieties, before analyzing the effect of protonation on the properties of the multi-Bodipy compound **1**, we performed an acid titration of its model species **5**.

The addition of acid to a solution of **5** in acetonitrile (concentration: 9.4×10^{-6} M) evidenced two consecutive processes: in the first one, until a 2:1 acid/**5** molar ratio was reached, several isosbestic points were maintained (Figure 10), and the main absorption modification took

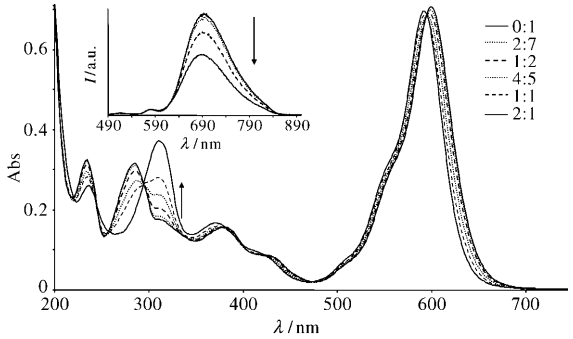

Figure 10. Absorption spectra changes of **5** upon protonation in acetonitrile. Concentration of **5** is 9.4×10^{-6} M; in the panel, the molar ratio between added triflic acid and **2** is reported. The inset shows the changes on emission spectra (excitation at an isosbestic point, 595 nm.)

place in the range 250–350 nm, which is the absorption range typical of spin-allowed π–π* transitions that involve bipyridine moieties.[39] In particular, the band maximizing at 287 nm in the starting compound moves to lower-energy and peaks at 315 nm upon acid addition. Simultaneously, there is only a small change in the emission spectrum shape, but the emission quantum yield decreases to 0.17 at the end of this titration step (it was 0.26 before acid addition; excitation wavelength was at 595 nm, at an isosbestic point). These data suggest that protonation does not take place at the amino group, but it involves the bipyridine moieties.[40] Also in this case, Specfit analysis indicates that two protons are involved: we assume that each proton is involved in the protonation of a single bipyridine molecule, with negligible interaction between the protonated sites. The global value for $\log k$ $(=\log k_1+\log k_2)$ for the **5**·$(2H)^{2+}$ species thus formed is 13.5 (with $(k_1+k_2)=3\times10^{13}\,M^{-2}$).

For acid/**5** molar ratios larger than 2:1, a further process, characterized by several isosbestics, takes place (see Figure SI-3 in the Supporting Information), which in any case requires a large excess amount of acid (about 100:1 acid/compound ratio) to be completed. In this successive process, the main spectral changes involve a (slight) blueshift of the low-energy absorption band, and a blueshift of the emission band, with enhanced emission quantum yield (Figure SI-3, inset). These changes can be rationalized on the assumption that further protonation of **5** takes place, and it involves the amino group.

With the information on the influence of acid addition on the properties of model **5** in our hands, we performed titration of **1** (concentration of **1**, 3.3×10^{-6} M). Similarly to what happens for **5**, for acid/compound ratios smaller than 2:1, a first process takes place in **1**; this process is clearly evidenced by several isosbestic points in the absorption spectra

and by a net change in the absorption spectrum area connected with bipyridine absorption (see Figure 11). Simultaneously, the low-energy emission at about 690 nm decreases

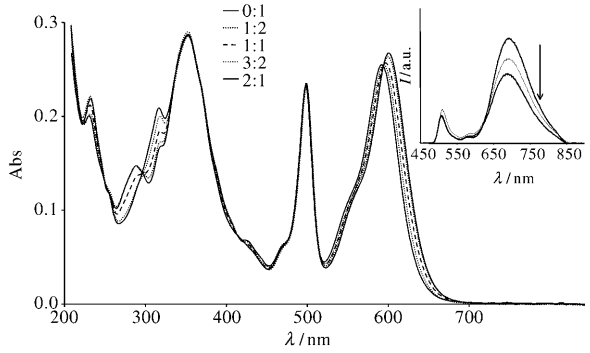

Figure 11. Absorption spectra changes of **1** upon protonation in acetonitrile. Concentration of **1** is 3.3×10^{-6} M; in the panel, the molar ratio between added triflic acid and **2** is reported. The inset shows the changes on emission spectra (excitation at an isosbestic point, 330 nm).

in intensity, reaching a quantum yield of 0.17 (in comparison to the original value of 0.26, see above). Interestingly, the high-energy emission at about 500 nm does not change appreciably during the titration (see Figure 11, inset). The titration process, by analogy with the changes occurring in **5**, can be identified as protonation of each bipyridine moiety. In the case of **1**, however, the rate constant and efficiency of the inter-Bodipy energy transfer are not significantly perturbed by protonation, which is different from that found for **2**. Specfit calculation yields a value of $\log k$ ($=\log k_1+\log k_2$) for the $\mathbf{1}\cdot(2\,\mathrm{H})^{2+}$ species thus formed of 13.1 (with $(k_1+k_2)=1.2\times10^{13}\,\mathrm{M}^{-2}$). Successively, a large excess of acid produces absorption changes that can be assigned to protonation of the aminostyryl group, with concomitant blueshift and enhancement of the low-energy emission (see Figure SI-4 in the Supporting Information).

The difference between **1** and **2**, as far as the influence of the initial protonation on the inter-Bodipy photoinduced energy transfer is concerned, would be connected with the changes in the (donor emission/acceptor absorption) spectral overlap J_F: protonation of the aminostyryl substituent of the acceptor dye in **2** induces a better spectral overlap J_F (it becomes $2.36\times10^{-13}\,\mathrm{cm}^6$, to be compared with the value of $1.12\times10^{-13}\,\mathrm{cm}^6$ of the unprotonated species mentioned above; see Figure 12), with a concomitant increased efficiency of the energy-transfer process. In **1**, the additional bipyridines efficiently compete with the amino group of the aminostyryl substituent for proton coordination, so that perturbation of the spectral overlap J_F results is negligible, at least for moderate acid/compound ratios (Figure 13), and as a consequence the effect of protonation on the energy-transfer efficiency is also negligible.

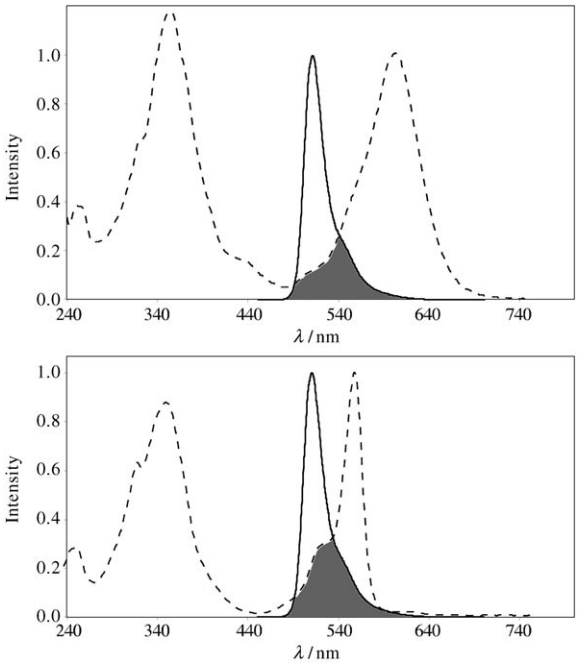

Figure 12. Illustration of modification in the spectral overlap integral J_F upon protonation of **2**. The solid line is the emission spectrum of the donor; the dashed line is the calculated absorption spectrum of the acceptor, obtained by subtracting the absorption spectrum of **2**—in its unprotonated (top) and protonated (bottom) forms—the absorption spectrum of **3**. Changes in the absorption spectrum area upon protonation are relevant.

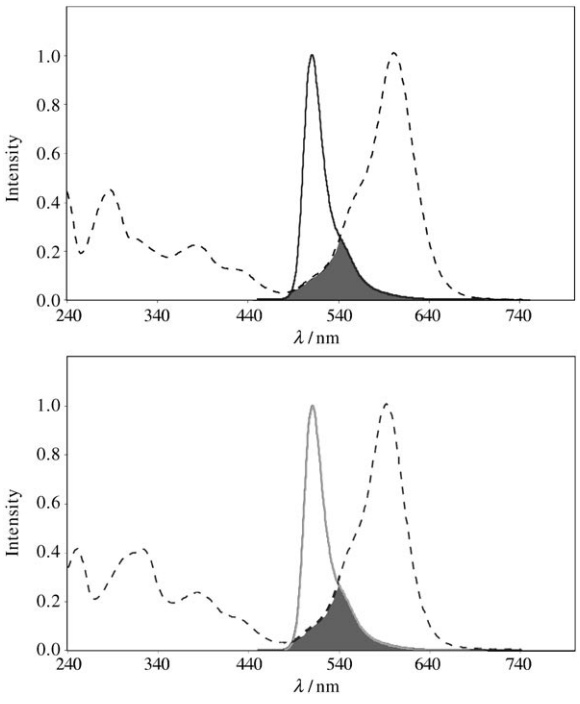

Figure 13. Illustration of modification in the spectral overlap integral J_F upon protonation in **1**. The solid line is the emission spectrum of the donor; the dashed line is the absorption spectrum of the acceptor (the spectra of unprotonated and protonated **7** are used to simulate the acceptor absorbance in **1**). Changes in the relevant absorption spectrum area were negligible. Compare with Figure 12.

Conclusion

Two new multichromophoric systems **1** and **2**, each one containing two different Bodipy dye subunits and one bridging fluorene species, have been prepared, along with two fluorene–Bodipy bichromophoric species, **6** and **7**, and three monomeric models, **3**, **4**, and **5**. The absorption spectra of the multichromophoric compounds are roughly the summation of the absorption spectra of the individual components, thereby demonstrating the supramolecular nature of the assemblies. Quantitative energy transfer from fluorene to Bodipy subunits occurs in **6** and **7**, and efficient (>90%) photoinduced energy transfer also occurs between the two Bodipy subunits of each multichromophoric species **1** and **2**, across the rigid fluorene bridge, with rate constants in the 10^9–10^{10} s^{-1} time range, by means of the Förster mechanism. Since some Bodipy dyes bear protonable groups such as aminostyryl substituents, and some of them also carry bipyridine groups, protonation has significant effects on the absorption spectra and luminescence properties of such species. More interestingly, the inter-Bodipy energy-transfer rate and efficiency in **2** increased upon the addition of acid, although at a moderate extent (about 40%), whereas acid addition has a negligible effect on the energy-transfer processes that occur in **1**, at least for low acid/**1** molar ratio (<2). This different behavior is due to the presence in **1** of bipyridine residues, which successfully compete with the aminostyryl moiety for protonation.

Although the effect of protonation on the inter-Bodipy energy transfer in **2** is moderate, this result suggests a possible way to control the interchromophoric energy-transfer efficiency in similar systems by means of a reversible external input, namely, protonation of the acceptor subunits.

Experimental Section

General: ^{1}H (200.1, 300.1, and 400 Hz) and ^{13}C (50.3, 75.5, and 100.3 Hz) NMR spectra were recorded at room temperature using the residual proton resonances in deuterated solvents as internal references. The high-resolution mass spectra were recorded using EI at 70 eV. Chromatographic purification was conducted using standardized silica gel 60 (0.063–0.200 mm). Thin-layer chromatography (TLC) was performed on silica gel plates coated with fluorescent indicator. All mixtures of solvents are given in v/v ratio. Absorption spectra were recorded using a JASCO V570 spectrophotometer. For luminescence spectra, a Jobin Yvon–Spex Fluoromax P spectrofluorimeter was used, equipped with a Hamamatsu R3896 photomultiplier, and the spectra were corrected for photomultiplier response using a program purchased with the fluorimeter. Luminescence lifetimes were determined by time-correlated single-photon counting (TCSPC) using an Edinburgh OB900 spectrometer (light pulse: Hamamatsu PL2 laser diode, pulse width 59 ps at 408 nm; or nitrogen discharge, pulse width at 337 nm: 2 ns). Luminescence quantum yields have been calculated by the optically diluted method[41] with $[Ru(bpy)_3]^{2+}$ (bpy = 2,2′-bipyridine) in air-equilibrated aqueous solution as the quantum yield standard (Φ = 0.028[42]). Time-resolved transient-absorption experiments were performed using a pump–probe setup based on the Spectra-Physics MAI-TAI Ti:sapphire system as the laser source and the Ultrafast Systems Helios spectrometer as the detector. The pump pulse was generated using a Spectra-Physics 800 FP OPA. The probe pulse was obtained by continuum generation on a sapphire plate (spectral range, 450–800 nm). Effective time resolution is around 200 fs; temporal chirp over the white-light 450–750 nm range is around 150 fs; and the temporal window of the optical delay stage is 0–3200 ps. The time-resolved data were analyzed using the Ultrafast Systems Surface Explorer Pro software.

Experimental uncertainties are as follows: absorption and luminescence maxima, 2 nm; emission quantum yields, 20%; emission lifetimes, 10%; transient absorption decay and rise rates, 10%.

Materials: 2,7-Dibromo-9,9-bis[2-(2-methoxyethoxy)ethyl]fluorene,[43] 8-(4-iodophenyl)-1,3,5,7-tetramethyl-4,4difluoro-4bora-3a,4a-diaza-*s*-indacene[23] were prepared according to the literature.

Synthesis of 2,7-di(trimethylsilylacetylene)-9,9-bis[2-(2-methoxyethoxy)-ethyl]fluorene: 2,7-Dibromo-9,9-bis[2-(2-methoxyethoxy)ethyl]fluorene (370 mg, 0.7 mmol) was dissolved in THF (20 mL) and triethylamine (5 mL) in a Schlenk tube. After bubbling argon through the mixture for 30 min, $[Pd(PPh_3)_2Cl_2]$ (50 mg, 0.07 mmol), trimethylsilylacetylene (0.3 mL, 2.1 mmol), and CuI (14 mg, 0.07 mmol) were added and the mixture stirred at room temperature for 48 h. The solvent was evaporated and the residue treated with dichloromethane, washed with water and brine, filtered over hydroscopic cotton wool, and rotary evaporated. The residue was purified by column chromatography on silica gel and eluted with ethyl acetate/petroleum ether (20:80 v/v) to give 2,7-di(trimethylsilylacetylene)-9,9-bis[2-(2-methoxyethoxy)ethyl]fluorene (162 mg, 40%) and 2-bromo-7-trimethylsilylacetylene-9,9-bis[2-(2-methoxyethoxy)ethyl]-fluorene (160 mg, 40%).

2,7-Di(trimethylsilylacetylene)-9,9-bis[2-(2-methoxyethoxy)ethyl]fluorene: ^{1}H NMR ($CDCl_3$, 200 MHz): δ = 0.28 (s, 18H), 2.38 (t, ^3J = 7.32 Hz, 4H), 2.69 (t, ^3J = 7.67 Hz, 4H) 3.12–3.17 (m, 4H), 3.26–3.31 (m, 10H) 7.51 ppm (AB system, J_{AB} = 7.63 Hz, $\upsilon_o\delta$ = 24.13 Hz, 4H); ^{13}C NMR ($CDCl_3$, 75 MHz): δ = 0.12, 39.72, 51.37, 59.13, 66.89, 70.06, 71.85, 95.09, 105.70, 120.05, 122.38, 127.02, 131.62, 140.17, 149.33 ppm; EIMS: *m*/*z* (%): 562.1 (100) $[M]^+$; elemental analysis calcd (%) for $C_{33}H_{46}O_4Si_2$ (M_r = 562.29): C 70.41, H 8.24; found: C 70.32, H 8.18.

2-Bromo-7-trimethylsilylacetylene-9,9-bis[2-(2-methoxyethoxy)ethyl]-fluorene: ^{1}H NMR ($CDCl_3$, 200 MHz): δ = 0.28 (s, 9H), 2.37 (t, ^3J = 7.49 Hz, 4H), 2.72 (t, ^3J = 7.49 Hz, 4H), 3.14–3.31 (m, 14H), 7.43–7.59 ppm (m, 6H); ^{13}C NMR ($CDCl_3$, 75 MHz): δ = 0.10, 39.64, 51.67, 59.13, 66.88, 70.06, 71.83, 95.05, 105.61, 119.81, 121.53, 121.91, 122.34, 126.90, 126.98, 130.74, 131.68, 138.83, 139.88, 148.66, 151.63 ppm; EIMS: *m*/*z* (%): 546.2 (100) $[M]^+$, 544.2 (100) $[M]^+$; elemental analysis calcd (%) for $C_{28}H_{37}BrO_4Si$ (M_r = 544.16): C 61.64, H 6.84; found: C 61.40, H 6.77.

Synthesis of compounds 4 and 4b: Compound 2,7-di(trimethylsilylacetylene)-9,9-bis[2-(2-methoxyethoxy)ethyl]fluorene (157 mg, 0.28 mmol) was dissolved in methyl alcohol (30 mL). K_2CO_3 (38 mg, 0.28 mmol) was added and the mixture was stirred at room temperature for 30 min. The mixture was then treated with water, extracted with dichloromethane, washed with brine, and filtered over hydroscopic cotton wool. After rotary evaporation the residue was purified by column chromatography on silica gel and eluted with ethyl acetate/petroleum ether (40:60 v/v) to give compounds **4b** (50 mg, 36%) and **4** (68 mg, 58%).

*Compound **4b***: ^{1}H NMR ($CDCl_3$, 200 MHz): δ = 0.27 (s, 9H), 2.37 (t, ^3J = 7.35 Hz, 4H), 2.70 (t, ^3J = 7.35 Hz, 4H), 3.13–3.30 (m, 14H), 7.43–7.61 ppm (m, 6H); ^{13}C NMR ($CDCl_3$, 75 MHz): δ = 0.10, 39.64, 51.40, 59.10, 66.89, 70.03, 71.82, 84.21, 95.14, 105.64, 120.11, 121.29, 122.47, 127.04, 124.14, 131.62, 131.77, 140.15, 140.47, 149.33, 149.45 ppm; EIMS: *m*/*z* (%): 490.1 (100) $[M]^+$; elemental analysis calcd (%) for $C_{30}H_{38}O_4Si$ (M_r = 490.25): C 73.43, H 7.41; found: C 73.59, H 7.63.

*Compound **4**:* ^{1}H NMR ($CDCl_3$, 200 MHz): δ = 2.37 (t, ^3J = 7.52 Hz, 4H), 2.73 (t, ^3J = 7.39 Hz, 4H), 3.13–3.30 (m, 14H), 7.54 ppm (AB system, J_{AB} = 7.93 Hz, $\upsilon_o\delta$ = 25.25 Hz, 4H); ^{13}C NMR ($CDCl_3$, 75 MHz): δ = 39.57, 51.44, 59.08, 66.91, 70,71.29, 84.16, 120.18 121.40, 127.17, 131.77, 140.33, 149.46 ppm; ESIMS: *m*/*z* (%): 418.1 (100) $[M]^+$; elemental analysis calcd (%) for $C_{27}H_{30}O_4$ (M_r = 418.21): C 77.48, H 7.22; found: C 77.27, H 7.04.

Synthesis of compounds 6 and 6b: 8-(4-Iodophenyl)-1,3,5,7-tetramethyl-4,4-difluoro-4-bora-3a,4a-diaza-*s*-indacene (90 mg, 0.21 mmol) and **4** (90 mg, 0.2 mmol) were dissolved in a mixture of benzene (20 mL) and

triethylamine (5 mL). Argon was bubbled through the mixture for 30 min. [Pd(PPh$_3$)$_4$] (25 mg, 0.02 mmol) was added and the mixture was stirred at 65 °C for 18 h. The solvent was then rotary evaporated and the residue treated with dichloromethane, washed with water and brine, filtered over hydroscopic cotton wool, and rotary evaporated. The residue was purified by column chromatography on silica gel and eluted with ethyl acetate/dichloromethane (10:90 v/v) to give compounds **6b** (50 mg) and **6** (33 mg).

Compound ***6b***: ^{1}H NMR ($CDCl_3$, 200 MHz): δ = 1.44 (s, 12H), 2.45–2.61 (m, 16H), 2.79 (t, ^3J = 7.30 Hz, 4H), 3.17–3.35 (m, 14H), 6.00 (s, 4H), 7.29–7.72 ppm (m, 14H); ^{13}C NMR ($CDCl_3$, 75 MHz): δ = 14.70, 29.80, 39.75, 51.49, 59.10, 67, 70.07, 71.83, 89.65, 91.45, 120.37, 121.50, 122.16, 124.19, 126.73, 128.42, 131.31, 132.42, 135.15, 140.27, 140.93, 143.12, 149.60, 155.89 ppm; ESIMS: *m*/*z* (%): 1062.2 (100) $[M]^+$; elemental analysis calcd (%) for $C_{65}H_{64}B_2F_4N_4O_4$ (M_r = 1062.5): C 73.45, H 6.07, N 5.27; found: C 73.12, H 5.62, N 5.09.

Compound ***6***: ^{1}H NMR ($CDCl_3$, 200 MHz): δ = 1.44 (s, 6H), 2.41 (t, ^3J = 7.30 Hz, 4H), 2.56 (s, 6H), 2.76 (t, ^3J = 7.30 Hz, 4H), 3.17–3.32 (m, 14H), 6 (s, 2H), 7.29–7.71 ppm (m, 10H); ^{13}C NMR ($CDCl_3$, 75 MHz): δ = 14.73, 29.83, 39.69, 51.50, 59.13, 66.98, 70.07, 71.85, 84.21, 89.60, 91.47, 120.21, 120.38, 121.46, 122.17, 124.22, 126.76, 127.20, 128.43, 131.28, 131.86, 132.44, 135.16, 140.26, 140.44, 140.96, 143.15, 149.46,149.66, 155.92 ppm; EIMS: *m*/*z* (%): 740.3 (100) $[M]^+$; elemental analysis calcd (%) for $C_{46}H_{47}BF_2N_2O_4$ (M_r = 740.36): C 74.59, H 6.40, N 3.78; found: C 74.38, H 6.18, N 3.56.

Synthesis of compound 1: Compounds **5** (85 mg, 96 μmol) and **6** (59 mg, 80 μmol) were dissolved in a mixture of benzene (20 mL) and triethylamine (5 mL). Argon was bubbled through the mixture for 30 min. [Pd(PPh$_3$)$_4$] (10 mg, 8 μmol) was added and the mixture was stirred at 65 °C for 18 h. The solvent was then rotary evaporated and the residue treated with dichloromethane, washed with water and brine, filtered over hydroscopic cotton wool, and rotary evaporated. The residue was purified by column chromatography on silica gel and eluted with dichloromethane/petroleum ether (60:40 v/v) to give compound **1** (50 mg). ^{1}H NMR (CD_2Cl_2, 400 MHz): δ = 1.45 (s, 3H), 1.48 (s, 9H), 2.39 (t, ^3J = 6.98 Hz, 4H), 2.50 (s, 9H), 2.79 (t, ^3J = 7.3 Hz, 4H), 3.13–3.24 (m, 16H), 5.00 (s, 4H), 5.99 (s, 1H), 6.02 (s, 2H), 6.59 (s, 1H), 7.21–7.82 (m, 28H), 8.30 (d, ^3J = 8 Hz, 2H), 8.41 (d, ^3J = 7.8 Hz, 2H), 8.63 ppm (d, ^3J = 3.7 Hz, 2H); ^{13}C NMR ($CDCl_3$, 75 MHz): δ = 14.63, 14.72, 15.02, 29.82, 39.78, 51.53, 57.58, 59.11, 67.03, 70.10, 71.86, 89.65, 89.80, 91.38, 91.51, 112.92, 115.14, 117.96, 119.70, 120.37, 120.85, 121.11, 121.38, 122.16, 122.25, 123.88, 124.02, 124.23, 125.85, 126.75, 128.45, 128.84, 129.48, 131.33, 132.31, 132.44, 132.95, 135.18, 135.59, 137.07, 137,54, 137.89, 138.27, 140.27, 140.33, 140.96, 142.71, 143.14, 149.33, 149.66, 153.71, 154.84, 155.92, 156.21, 156.33, 157.88 ppm; EIMS: *m*/*z* (%): 1501.5 (100) $[M]^+$; elemental analysis calcd (%) for $C_{94}H_{85}B_2F_4N_9O_4$ (M_r = 1501.68): C 75.15, H 5.10, N 8.39; found: C 74.87, H 5.44, N 8.19.

Synthesis of compound 7: Compounds **5** (98 mg, 0.11 mmol) and **4b** (45 mg, 92 μmol) were dissolved in a mixture of benzene (20 mL) and triethylamine (5 mL). Argon was bubbled through the mixture for 30 min. [Pd(PPh$_3$)$_4$] (10 mg, 8 μmol) was added and the mixture was stirred at 65 °C for 18 h. The solvent was then rotary evaporated and the residue treated with dichloromethane, washed with water and brine, filtered over hydroscopic cotton wool, and rotary evaporated. The residue was purified by column chromatography on alumina and eluted with dichloromethane (100%) to give compound **7** (40 mg, 40%). ^{1}H NMR ($CDCl_3$, 300 MHz): δ = 0.28 (s, 9H), 1.47 (s, 3H), 1.50 (s, 3H), 2.43 (t, ^3J = 7.3 Hz, 4H), 2.55 (s, 3H), 2.75 (t, ^3J = 7.3 Hz, 4H), 3.16–3.31 (m, 16H), 5.00 (s, 4H), 5.97 (s, 1H), 6.58 (s, 1H), 7.15–7.33 (m, 8H, overlap with solvent), 7.45–7.86 (m, 16H), 8.32 (d, ^3J = 7.9 Hz, 2H), 8.41 (d, ^3J = 7.9 Hz, 2H), 8.70 ppm (d, ^3J = 4.1 Hz, 2H); ^{13}C NMR ($CDCl_3$, 400 MHz): δ = 0.13, 14.19, 14.64, 15.04, 22.48, 34.28, 39.78, 51.47, 57.60, 59.14, 66.98, 70.10, 71.88, 89.69, 91.44, 105.70, 112.95, 117.96, 119.87, 120.11, 120.32, 121.29, 121.58, 122.13, 122.52, 123.99, 124.08, 125.95, 126.75, 127.07, 128.84, 129.49, 131.27, 131.71, 132.33, 135.57, 137.48, 138, 140.17, 140.35, 142.29, 142.75, 149.05, 149.37, 149.66, 153.75, 154.83, 155.98, 157.97 ppm; EIMS: *m*/*z* (%): 1193.4 (100) $[M]^+$; elemental analysis calcd (%) for $C_{78}H_{76}BF_2N_7O_4Si$ (M_r = 1193.58): C 74.44, H 6.16, N 5.87; found: C 74.13, H 6.36, N 5.71.

Synthesis of compound 2: In a round-bottomed flask equipped with a Dean Stark apparatus, 4-dimethylaminobenzaldehyde (8 mg, 0.06 mmol) and piperidine (2 mL) were added to a stirred solution of compound **6b** (69 mg , 0.06 mmol) in toluene (20 mL). The solution was heated at reflux during 12 h. After cooling to room temperature, the mixture was washed with water and brine. The organic phase was filtered over hydroscopic cotton wool and rotary evaporated. The residue was purified by column chromatography on silica gel eluting with a gradient of ethyl acetate/petroleum ether (20:80 to 60:40) to give compound **2** (32 mg, 45%). ^{1}H NMR (CD_2Cl_2, 400 MHz): δ = 1.47 (s, 3H), 1.51 (s, 6H), 2.41 (t, ^3J = 7.38 Hz, 4H), 2.52 (s, 6H), 2.55 (s, 3H), 2.82 (t, ^3J = 7.18 Hz, 4H), 3.03 (s, 6H), 3.16–318 (m, 4H), 3.22 (s, 6H), 3.24–3.27 (m, 6H), 6.02 (s, 1H), 6.04 (s,1H), 6.65 (s, 1H), 6.71 (d, ^3J = 9 Hz, 2H), 7.24 (d, ^3J = 15.9 Hz, 1H), 7.33–7.39 (m, 5H), 7.50 (d, ^3J = 9 Hz, 2H), 7.59 (dt, ^3J = 7.8 Hz, ^4J = 1.64 Hz, 2H), 7.68–7.75 ppm (m, 8H); ^{13}C NMR ($CDCl_3$, 400 MHz): δ = 14.56, 15.65, 14.97, 39.69, 51.42, 59.04, 66.92, 70.01, 71.77, 89.56, 89.71, 91.29, 91.40, 117.93, 120.28, 120.80, 121.42, 122.06, 122.15, 123.93, 124.12, 126.65, 128.34, 128.75, 129.33, 131.25, 132.23, 132.34, 132.91, 135.07, 135.47, 140.17, 140.23, 140.86, 142.63, 143.06, 149.52, 155.82 ppm; ESIMS: *m*/*z* (%): 1193.4 (100) $[M]^+$; elemental analysis calcd (%) for $C_{74}H_{73}B_2F_4N_5O_4$ (M_r = 1193.58): C 74.44, H 6.16, N 5.87; found: C 74.21, H 5.72, N 5.59.

Acknowledgements

The authors thank the University of Messina (Progetti di Ricerca di Ateneo, PRA), the International Centre for Tropical Agriculture (CIAT) laboratory of the University of Messina, the MIUR (PRIN projects), and the Centre national de la Recherche Scientifique for financial support and research facilities.

[1] The literature on this topic is too vast to be exhaustively quoted. For some representative recent books or reviews, see: a) V. Balzani, F. Scandola, F. *Supramolecular Photochemistry*, Horwood, Chichester, **1991**, Chapter 6; b) B. V. Van der Meer, G. Coker III, S.-Y. S. Chen, *Resonance Energy Transfer: Theory and Data*, Wiley-VCH, Weinheim, **1994**; c) T. Pullerits, V. Sundström, *Acc. Chem. Res.* **1996**, *29*, 381; d) S. E. Braslavsky, *Pure Appl. Chem.* **2007**, *79*, 293, and references therein.

[2] a) R. Amadelli, R. Argazzi, C. A. Bignozzi, F. Scandola, *J. Am. Chem. Soc.* **1990**, *112*, 7099; b) T. A. Heimer, E. J. Heilweil, C. A. Bignozzi, G. J. Meyer, *J. Phys. Chem. A* **2000**, *104*, 4256; c) B. O'Regan, M. Grätzel, *Nature* **1991**, *353*, 737; d) M. Grätzel, *J. Photochem. Photobiol. C* **2003**, *4*, 145; e) M. Grätzel, *Inorg. Chem.* **2005**, *44*, 6841; f) S. Ardo, G. J. Meyer, *Chem. Soc. Rev.* **2009**, *38*, 115, and refs. therein.

[3] a) D. Holten, D. F. Bocian, J. S. Lindsey, *Acc. Chem. Res.* **2002**, *35*, 57; b) M. Hambourger, G. F. Moore, D. M. Kramer, D. Gust, A. L. Moore, T. A. Moore, *Chem. Soc. Rev.* **2009**, *38*, 25; c) G. Calzaferri, O. Bossarto, S. Bruhwiler, C. Huber, C. Leiggener, M. K. Van Veek, A. Z. Ruiz, *C. R. Chim.* **2006**, *9*, 214; d) J. H. Alstrum-Acevedo, M. K. Brennaman, T. J. Meyer, *Inorg. Chem.* **2005**, *44*, 6802; e) M. R. Wasielewski, *Acc. Chem. Res.* **2009**, *42*, 1910; f) J. J. Concepcion, J. W. Jurss, M. K. Brennaman, P. G. Hoertz, A. O. T. Patrocinio, N. Y. Murakami Iha, J. L. Templeton, T. J. Meyer, *Acc. Chem. Res.* **2009**, *42*, 1954.

[4] a) S. Serroni, S. Campagna, R. Pistone Nascone, G. S. Hanan, G. J. Davidson, J.-M. Lehn, *Chem. Eur. J.* **1999**, *5*, 3523; b) D. J. Cárdenas, J.-P. Collin, P. Gavina, J.-P. Sauvage, A. De Cian, J. Fischer, N. Armaroli, L. Flamigni, V. Vicinelli, V. Balzani, *J. Am. Chem. Soc.* **1999**, *121*, 5481; c) N. Armaroli, J.-F. Eckert, J.-F. Nierengarten, *Chem. Commun.* **2000**, 2105; d) M. T. Indelli, M. Ghirotti, A. Prodi, C. Chiorboli, F. Scandola, N. D. McClenaghan, F. Puntoriero, S. Campagna, *Inorg. Chem.* **2003**, *42*, 5489; e) D. Bonifazi, M. Scholl, F. Y.

Song, L. Echegoyen, G. Accorsi, N. Armaroli, F. Diederich, *Angew. Chem.* **2003**, *115*, 5116; *Angew. Chem. Int. Ed.* **2003**, *42*, 4966; f) G. Accorsi, N. Armaroli, *J. Phys. Chem. C* **2010**, *114*, 1385.

[5] For some examples, see: a) T. J. Meyer, *Acc. Chem. Res.* **1989**, *22*, 163; b) M. R. Wasielewski, *Chem. Rev.* **1992**, *92*, 435; c) V. Balzani, S. Campagna, G. Denti, A. Juris, S. Serroni, M. Venturi, *Acc. Chem. Res.* **1998**, *31*, 26; d) K. Kilsá, J. Kajanus, J. Mårtersson, B. Albinsson, *J. Phys. Chem. B* **1999**, *103*, 7329; e) A. El-ghayoury, A. Harriman, A. Khatyr, R. Ziessel, *J. Phys. Chem. A* **2000**, *104*, 1512; f) A. Harriman, A. Khatyr, R. Ziessel, A. C. Benniston, *Angew. Chem.* **2000**, *112*, 4457; *Angew. Chem. Int. Ed.* **2000**, *39*, 4287; g) D. Gust, T. A. Moore, A. L. Moore, *Acc. Chem. Res.* **2001**, *34*, 40; h) A. Tsuda, A. Osuka, *Science* **2001**, *293*, 79; i) F. Würthner, *Chem. Commun.* **2004**, 1564; j) F. Puntoriero, S. Serroni, M. Galletta, A. Juris, A. Licciardello, C. Chiorboli, S. Campagna, F. Scandola, *ChemPhysChem* **2005**, *6*, 129; k) A. Prodi, C. Chiorboli, F. Scandola, E. Iengo, E. Alessio, *ChemPhysChem* **2006**, *7*, 1514; l) J. Larsen, F. Puntoriero, T. Pascher, N. D. McClenaghan, S. Campagna, E. Åkesson, V. Sundström, *ChemPhysChem* **2007**, *8*, 2643; m) B. Albinsson, J. Mårtersson, *J. Photochem. Photobiol. C* **2008**, *9*, 138; n) B. Ventura, A. Barbieri, F. Barigelletti, J. B. Seneclauze, P. Retailleau, R. Ziessel, *Inorg. Chem.* **2008**, *47*, 7048; o) J.-L. Wang, J. Yan, Z.-M. Tang, Q. Xiao, Y. Ma, J. Pei, *J. Am. Chem. Soc.* **2008**, *130*, 9952.

[6] a) H. McConnell, *J. Chem. Phys.* **1961**, *35*, 508; b) M. N. Paddon-Row in *Electron Transfer in Chemistry, Vol. 3* (Ed.: V. Balzani), Wiley-VCH, Weinheim, **2001**, p. 179.

[7] D. L. Dexter, *J. Chem. Phys.* **1953**, *21*, 836.

[8] a) B.-J. Jung, J.-I. Lee, H. Y. Chu, L.-M. Do, H.-K. Shim, *Macromolecules* **2002**, *35*, 2282; b) S. Inaoka, R. Advincula, *Macromolecules* **2002**, *35*, 2426; c) M. S. Liu, X. Jiang, S. Liu, P. Herguth, A. K.-Y. Jen, *Macromolecules* **2002**, *35*, 3532; d) W.-L. Yu, J. Pei, Y. Cao, W. Huang, A. J. Heeger, *Chem. Commun.* **1999**, 1837; e) N. G. Pschirer, U. H. F. Bunz, *Macromolecules* **2000**, *33*, 3961.

[9] O. Inganas, F. Zhang, M. R. Andersson, *Acc. Chem. Res.* **2009**, *42*, 1713.

[10] a) U. Scherf, E. J. M. List, *Adv. Mater.* **2002**, *14*, 477; b) M. Leclerc, *J. Polym. Sci. Polym. Chem. Ed.* **2001**, *39*, 2867; c) S. Setayesh A. C. Grimsdale, T. Weil, V. Enkelmann, K. Müllen, F. Meghdadi, E. J. W. List, G. Leising, *J. Am. Chem. Soc.* **2001**, *123*, 946; d) D. Marsitzky, R. Vestberg, P. Blainey, B. T. Tang, C. J. Hawker, K. R. Carter, *J. Am. Chem. Soc.* **2001**, *123*, 6965; e) W.-L. Yu, J. Pei, W. Huang, A. J. Heeger, *Adv. Mater.* **2000**, *12*, 828; f) W.-L. Yu, Y. Cao, J. Pei, W. Huang, A. J. Heeger, *Appl. Phys. Lett.* **1999**, *75*, 3271.

[11] J. B. Seneclauze, P. Retailleau, R. Ziessel, *New J. Chem.* **2007**, *31*, 1412.

[12] a) R. Ziessel, G. Ulrich, A. Harriman, *New J. Chem.* **2007**, *31*, 496; b) R. Ziessel, *C. R. Acad. Sci. Chim.* **2007**, *10*, 622; c) G. Ulrich, R. Ziessel, A. Harriman, *Angew. Chem.* **2008**, *120*, 1202; *Angew. Chem. Int. Ed.* **2008**, *47*, 1184; d) A. Loudet, K. Burgess, *Chem. Rev.* **2007**, *107*, 4891.

[13] A. Harriman, L. J. Mallon, K. J. Elliot, A. Haefele, G. Ulrich, R. Ziessel, *J. Am. Chem. Soc.* **2009**, *131*, 13375.

[14] S. Diring, F. Puntoriero, F. Nastasi, S. Campagna, R. Ziessel, *J. Am. Chem. Soc.* **2009**, *131*, 6108.

[15] a) S. Hattori, K. Ohkubo, Y. Urano, H. Sunahara, T. Nagano, Y. Wada, N. V. Tkachenko, H. Lemmetyinen, S. Fukuzumi, *J. Phys. Chem. B* **2005**, *109*, 15368; b) S. Erten-Ela, D. Yilmaz, B. Icli, Y. Dede, S. Icli, E. U. Akkaya, *Org. Lett.* **2008**, *10*, 3299; c) T. Rousseau, A. Cravino, J. Roncali, T. Bura, G. Ulrich, R. Ziessel, *Chem. Commun.* **2009**, 1673; d) T. Rousseau, A. Cravino, J. Roncali, T. Bura, G. Ulrich, R. Ziessel, *J. Mater. Chem.* **2009**, *19*, 2298; e) D. Kumaresan, R. P. Thummel, T. Bura, G. Ulrich, R. Ziessel, *Chem. Eur. J.* **2009**, *15*, 6335.

[16] a) N. R. Cha, S. Y. Moon, S. K. Chang, *Tetrahedron Lett.* **2003**, *44*, 8265; b) N. Basaric, M. Baruah, W. Qin, B. Metten, M. Smet, W. Dehaen, N. Boens, *Org. Biomol. Chem.* **2005**, *3*, 2755; c) H. J. Kim, J. S. Kim, *Tetrahedron Lett.* **2006**, *47*, 7051; d) C. Goze, G. Ulrich, L. Charbonnière, R. Ziessel, *Chem. Eur. J.* **2003**, *9*, 3748; e) B. Ventura, G. Marconi, M. Bröning, R. Krüger, L. Flamigni, *New J. Chem.* **2009**, *33*, 428.

[17] R. P. Haughland, *Handbook of Fluorescent Probes and Research Products*, 9th ed., Molecular Probes, Eugene, **2002**, pp. 36–46.

[18] a) F. López Arbeloa, J. Banuelos Prieto, V. Martinez Martinez, T. Arbeloa Lopez, I. Lopez Arbeloa, *ChemPhysChem* **2004**, *5*, 1762; b) S. Mula, A. K. Ray, M. Banerjee, T. Chaudhuri, K. Dasgupta, S. Chattopadhyay, *J. Org. Chem.* **2008**, *73*, 2146.

[19] P. Didier, G. Ulrich, Y. Mély, R. Ziessel, *Org. Biomol. Chem.* **2009**, *7*, 3639.

[20] F. Camerel, L. Bonardi, G. Ulrich, L. Charbonnière, B. Donnio, C. Bourgogne, D. Guillon, P. Retailleau, R. Ziessel, *Chem. Mater.* **2006**, *18*, 5009.

[21] F. Camerel, L. Bonardi, M. Schmutz, R. Ziessel, *J. Am. Chem. Soc.* **2006**, *128*, 4548.

[22] a) A. Nagai, J. Miyake, K. Kokado, Y. Nagata, Y. Chujo, *J. Am. Chem. Soc.* **2008**, *130*, 15276; b) A. Nagai, Y. Chujo, *Macromolecules* **2010**, *43*, 193.

[23] a) G. Ulrich, R. Ziessel, *J. Org. Chem.* **2004**, *69*, 2070; b) L. Bonardi, G. Ulrich, R. Ziessel, *Org. Lett.* **2008**, *10*, 2183.

[24] T. Bura, R. Ziessel, *Tetrahedron Lett.* **2010**, *51*, 2875.

[25] E. Knoevenagel, *Ber. Dtsch. Chem. Ges.* **1898**, *31*, 2596.

[26] a) R. P. Haughland, H. C. Kang, U.S. Patent 4,774,339, **1988**; b) K. Rurack, M. Kollmansberger, J. Daub, *New J. Chem.* **2001**, *25*, 289; c) Z. Dost, S. Atilgan, E. U. Akkaya, *Tetrahedron* **2006**, *62*, 8484; d) S. Atilgan, Z. Ekmekci, A. L. Dogan, D. Guc, E. U. Akkaya, *Chem. Commun.* **2006**, 4398.

[27] A. Coskun, E. U. Akkaya, *J. Am. Chem. Soc.* **2006**, *128*, 14474–14475.

[28] R. Ziessel, G. Ulrich, A. Harriman, M. A. H. Alamiry, B. Stewart, P. Retailleau, *Chem. Eur. J.* **2009**, *15*, 1359–1369.

[29] M. Baruah, W. W. Qin, C. Flors, J. Hofkens, R. A. L. Vallée, D. Beljonne, M. Van der Auweraer, W. M. De Borggraeve, N. Boens, *J. Phys. Chem. A* **2006**, *110*, 5998.

[30] For unquenched quantum yield and lifetimes, we consider here the values of **6** and for the quenched figures we consider the quantum yields and lifetimes (on exciting at a wavelength at which absorption of the higher-energy Bodipy is maximized, that is, 480 nm) of the high-energy emission of **1** and **2**.

[31] It can be noted that the rate constants calculated by Equation (2) are always slightly larger than those calculated by Equation (1). This could be due to the presence of trace impurities of starting compounds missing the acceptor subunits. Please note that traces of such impurities, even under the level of detection by any other method, could affect the quantum yield data, whereas they do not affect the lifetime data, which are therefore considered to be more reliable values.

[32] Th. Förster, *Discuss. Faraday Soc.* **1959**, *27*, 7.

[33] a) L. De Cola, V. Balzani, F. Barigelletti, L. Flamigni, P. Belser, A. Von Zelewsky, M. Frank, F. Vögtle, *Inorg. Chem.* **1993**, *32*, 5228; b) F. Barigelletti, L. Flamigni, *Chem. Soc. Rev.* **2000**, *29*, 1.

[34] S. E. Braslavsky, E. Fron, H. B. Rodriguez, E. San Roman, G. D. Scholes, G. Schwltzer, B. Valeur, J. Wirz, *Photochem. Photobiol. Sci.* **2008**, *7*, 1444, and references therein.

[35] A. Harriman, L. Mallon, R. Ziessel, *Chem. Eur. J.* **2008**, *14*, 11461.

[36] Energy-transfer rate constants calculated by Equation (3) have also led to values larger than experimental ones for other systems in which aminostyryl-substituted Bodipy molecules—and as a consequence CT states—were involved.[14]

[37] E. Deniz, G. C. Isbasar, O. A. Bozdemir, L. T. Yildirim, A. Siemiarczuk, E. U. Akkaya, *Org. Lett.* **2008**, *10*, 3401, and references therein.

[38] Besides reducing the energy-transfer driving force, by increasing the excited-state level of the acceptor chromophore, the blueshift of the absorption band of the amino-styryl-substituted Bodipy (i.e., the acceptor partner of the energy-transfer process) upon protonation modifies the spectral overlap J_F between donor emission and acceptor absorption spectra.

[39] a) A. Juris, V. Balzani, F. Barigelletti, S. Campagna, P. Belser, A. von Zelewsky, *Coord. Chem. Rev.* **1988**, *84*, 85; b) J.-P. Sauvage, J.-P.

Collin, J.-C. Chambron, S. Guillerez, C. Coudret, V. Balzani, F. Barigelletti, L. De Cola, L. Flamigni, *Chem. Rev.* **1994**, *94*, 993; c) V. Balzani, A. Juris, M. Venturi, S. Campagna, S. Serroni, *Chem. Rev.* **1996**, *96*, 759.

[40] The decreased emission quantum yield of the protonated chromophore relative to the unprotonated species could be due to effective participation of the protonated bipyridine moiety in the radiationless decay. However, this aspect is not investigated here.

[41] J. N. Demas, G. A. Crosby, *J. Phys. Chem.* **1971**, *75*, 991.

[42] K. Nakamaru, *Bull. Chem. Soc. Jpn.* **1982**, *55*, 2697.

[43] S. Gug, F. Bolze, A. Specht, C. Bourgogne, M. Goeldner, J.-F. Nicoud, *Angew. Chem.* **2008**, *120*, 9667; *Angew. Chem. Int. Ed.* **2008**, *47*, 9525.

Received: February 22, 2010
Published online: June 23, 2010

